97-111

Environment Canada / Environnement Canada

Canada

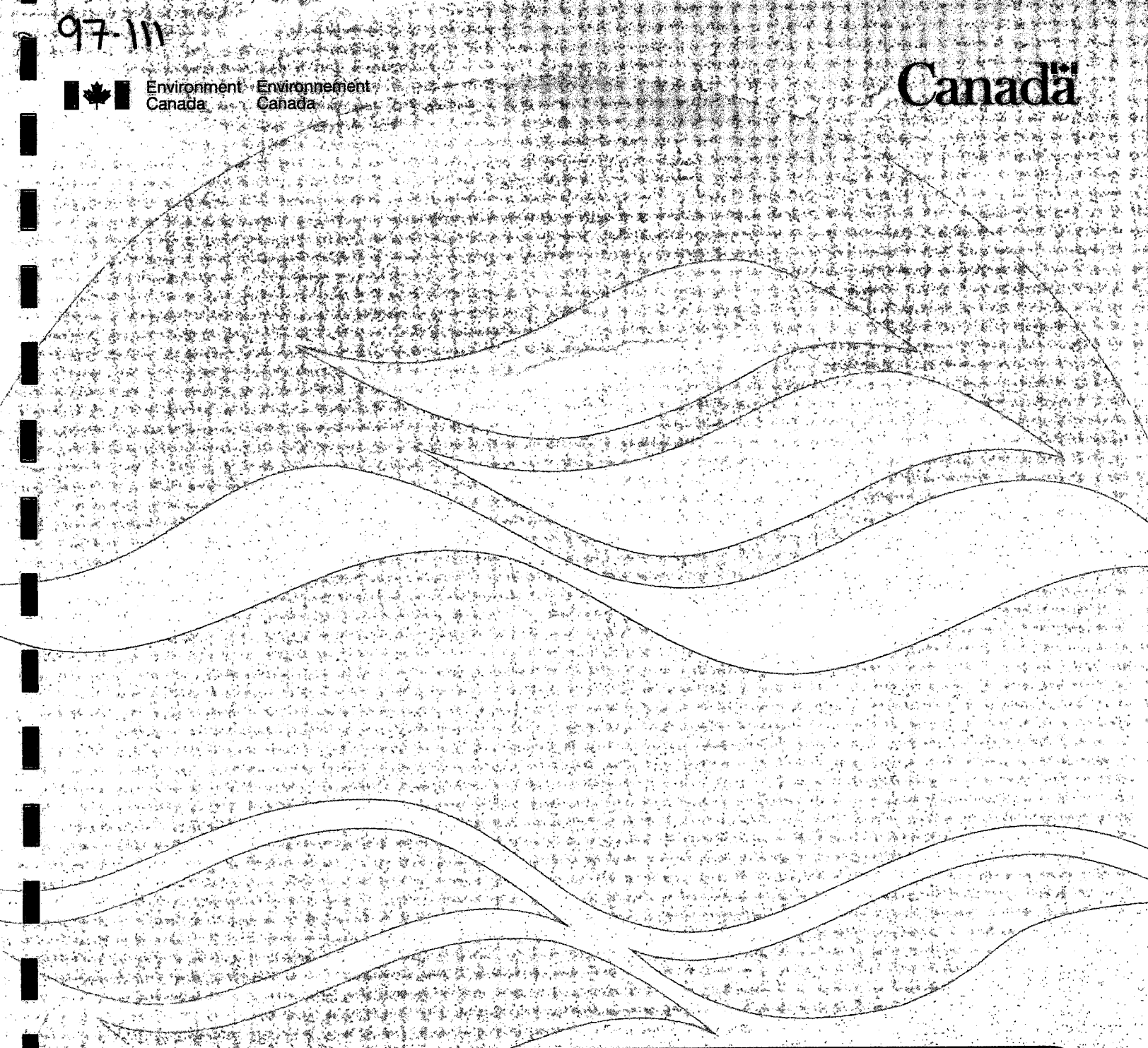

A Model For Slug Tests Conducted In Vertically Fractured Media

By:

J. M. Markle, K.S. Novakowski, R.K. Rowe

NWRI Contribution No: 97-111

NATIONAL WATER RESEARCH INSTITUTE

INSTITUT NATIONAL DE RECHERCHE SUR LES EAUX

A MODEL FOR SLUG TESTS CONDUCTED IN VERTICALLY FRACTURED MEDIA

BY

J.M. MARKLE[1], K.S. NOVAKOWSKI[2], AND R.K. ROWE[1]

NWRI Contribution # 97-111

For submission to:
WATER RESOURCES RESEARCH

January, 1997

[1] University of Western Ontario, London, Ontario.
[2] National Water Research Institute, Burlington, Ontario.

MANAGEMENT PERSPECTIVE

Title: **A MODEL FOR SLUG TESTS CONDUCTED IN VERTICALLY FRACTURED MEDIA**

Author(s): J. Markle, K. Novakowski and R.K. Rowe

NWRI Publ. #: 97-111

Citation: To be Submitted to Water Resources Research

EC Priority/Issue: In many clay environments in southern Ontario, hazardous waste facilities are sited because the clay is assumed to offer some protection to underlying water supplies. Most clays in southern Ontario, however, are pervaded by vertical fractures that form either due to dessication or through neo-tectonic forces. These fractures may be limited to the upper horizons of the clay or they may penetrate the entire clay formation. To properly estimate the potential for groundwater movement and contaminant migration through these fractures, accurate estimates of the hydraulic properties of the fractures are necessary. This paper describes the development and use of a mathematical model for the interpretation of a hydraulic test conducted where the measuring device intersects a vertical fracture. Estimates of error indicate that by not using this model for interpretation, significant error in the estimate of contaminant movement could be incurred. Thus, the EC issue addressed by this study is toxics in groundwater.

Current Status: Continuing work on this model is not currently planned.

Next Steps: Study is complete.

1. Introduction

Geological formations having moderate to low permeability such as crystalline and argillaceous rocks, and unconsolidated formations such as clay, are often considered to be good barriers to contaminant migration. However, vertical or sub-vertical fractures and joints of significant permeability often occur in these types of media [ie. *Grisak and Cherry*, 1975; *Keller et al.*, 1986; *Raven*, 1986; and *D'Astous et al.*, 1988]. These fractures and joints may be the main conduits for the flow of water and they can significantly influence the bulk permeability of the formation [*Neuzil and Tracy*, 1981; *McKay et al.*, 1993; and *Hinsby et al.*, 1996]. Results from several investigations indicate that vertical fractures are the controlling feature in the transport of contaminants through fractured aquitards [*Roberts et al.*, 1982; *Rudolph et al.*, 1991; and *Sudicky and McLaren*, 1992]. The proper determination of the hydraulic properties of these fractures is critical to assessing groundwater flow and transport in these formations.

The slug test is a commonly used hydraulic testing method that involves inducing a head or pressure disturbance in the wellbore and measuring the decay in the hydraulic head response. From these measurements the hydraulic properties of the formation can be estimated using one of the several curve fitting methods that have been developed for interpreting slug tests. However, in fractured formations the interpretation of results from a slug test may be complicated by the presence of a vertical fracture. As well, drilling and well completion practices may alter the hydraulic properties of the fracture near the wellbore. This altered zone may be treated as a skin of finite thickness and it's influence on the test may further complicate

the interpretation. Therefore a method of interpreting slug tests influenced by these factors would be advantageous.

Numerous analytical models have been developed for the interpretation of slug tests conducted in radial flow conditions [ie. *Cooper et al.*, 1967; *Bredehoeft and Papadopulos*, 1980; *Barker and Black*, 1983; *Dougherty and Babu*, 1984; *Moench and Hsieh*, 1985; *Grader and Ramey*, 1988; and *Hyder et al.*, 1994]. These models range in complexity accounting for a combination of conditions such as the presence of a skin of finite thickness, horizontal fractures, a partially penetrating well, and a formation having dual porosity. However, none are suitable for the interpretation of slug tests influenced by the presence of a vertical fracture.

Several analytical models for the constant flow rate test in wells completed in media having vertical fractures are found in the petroleum literature [*Prats*, 1962; *Gringarten et al.*, 1974; *Cinco-Ley et al.*, 1978; and *Cinco-Ley and Samaniego-V.*, 1981]. These models are based on the fissure block model in which the flow from a porous reservoir into a vertical fracture whose plane intersects the axis of the well, is considered. The influence of a finite-thickness skin and partial penetration are not incorporated. *Karasaki et al.* [1988] gives the solution for a slug test in a fully penetrating well intersecting a single vertical fracture. The presence of a skin and a permeable matrix were not considered in this solution.

This paper presents a semi-analytical model that can be used in the interpretation of slug tests conducted in vertically fractured media. The model is based on bilinear flow theory in

which transient, linear flow in both the fracture and the matrix is considered. Therefore it is an extension to the linear flow model presented by *Karasaki et al.* [1988]. Using the model we develop interpretation techniques for early, intermediate, and late time data. We present type curves for each of these time periods, and investigate both the effects of the various features of the model and the practical implications on the interpretation of test data. We discuss the similarities between the linear, bilinear, and radial flow type curves and develop criteria which define the conditions under which unique type curve matches can be assured. Finally, we discuss the error that may result if tests influenced by either linear or bilinear flow are interpreted using the *Cooper et al.* [1967] radial flow model.

2. Mathematical Model

Figure 1 shows a schematic diagram illustrating the boundary value problem to be considered. The fracture is semi-infinite in lateral extent, of finite hydraulic conductivity, fully confined and characterized by two smooth parallel plates. All flow across the open interval of the partially penetrating wellbore occurs through the fracture, and there is an exchange of water between the fracture and the porous matrix. Two-dimensional, linear flow is assumed in the anisotropic matrix with flow restricted to the vertical direction and the horizontal direction normal to the plane of the fracture. It is reasonable to neglect horizontal flow parallel to the fracture plane, as is done here, provided that the hydraulic diffusivity of the fracture is two orders of magnitude greater than that of the matrix [*Kissling and Young,* 1989]. Finally, consideration is given to the presence of a finite thickness skin located immediately adjacent to

the wellbore, and having hydraulic properties different from the fracture.

The governing differential equation describing two-dimensional, transient flow in the skin and the fracture is the linear flow equation with a sink term for the matrix and is given by

$$\frac{\partial^2 h_i(x,z,t)}{\partial x^2}+\frac{\partial^2 h_i(x,z,t)}{\partial z^2}+\frac{2K_{Y_3}}{K_i e_i}\frac{\partial h_3}{\partial y}\bigg|_{y=0}=\frac{S_{S_i}}{K_i}\frac{\partial h_i(x,z,t)}{\partial t} \qquad \begin{matrix} i=1 & r_w\le x\le x_1 \\ i=2 & x_1\le x\le\infty \\ & 0\le y\le\infty \\ & 0\le z\le L \end{matrix} \tag{1}$$

where subscript *1* denotes the skin zone, subscript *2* denotes the fracture zone, h_i, K_i, S_{S_i}, and e_i ($i=1,2$) are the hydraulic head, hydraulic conductivity, specific storage, and aperture of the skin and fracture respectively, h_3 is the hydraulic head in the matrix, and K_{Y_3} is the lateral hydraulic conductivity of the matrix. The initial condition for the fracture and skin zone is

$$h_1(x,z,0)=h_2(x,z,0)=h_0 \tag{2}$$

The outer boundary condition for the fracture is

$$h_2(\infty,z,t)=h_0 \tag{3}$$

The upper and lower boundary conditions in the z-direction are

$$\frac{\partial h_1(x,L,t)}{\partial z}=\frac{\partial h_2(x,L,t)}{\partial z}=0 \tag{4}$$

$$\frac{\partial h_1(x,0,t)}{\partial z}=\frac{\partial h_2(x,0,t)}{\partial z}=0 \tag{5}$$

Continuity between the skin zone and the fracture requires that

$$h_1(x_1,z,t)=h_2(x_1,z,t) \tag{6}$$

$$K_1 e_1 \frac{\partial h_1(x_1,z,t)}{\partial x} = K_2 e_2 \frac{\partial h_2(x_1,z,t)}{\partial x} \tag{7}$$

The governing differential equation describing two-dimensional flow in the matrix is

$$K_{Y_3} \frac{\partial^2 h_3}{\partial y^2} + K_{Z_3} \frac{\partial^2 h_3}{\partial z^2} = S_{S_3} \frac{\partial h_3}{\partial t} \tag{8}$$

where K_{Z_3} and S_{S_3} are the vertical hydraulic conductivity and the specific storage of the matrix, respectively. The initial condition is

$$h_3(x,y,z,0)=h_0 \tag{9}$$

The boundary conditions are

$$h_3(x,\infty,z,t)=h_0 \tag{10}$$

$$\frac{\partial h_3(x,y,0,t)}{\partial z} = \frac{\partial h_3(x,y,L,t)}{\partial z} = 0 \tag{11}$$

$$h_3(x,0,z,t)=h_1(x,z,t) \qquad r_w \le x \le x_1 \tag{12}$$

$$h_3(x,0,z,t)=h_2(x,z,t) \qquad x_1 \le x \le \infty \tag{13}$$

In this model the flux across the open interval of the wellbore occurs only through the fracture. In addition, a constant hydraulic gradient is assumed within the well screen so that the flux along the open interval is independent of z. Therefore, the mass balance equation for the partially penetrating well is given by

$$2K_1 e_1 b \left.\frac{\partial h_1(x,z,t)}{\partial x}\right|_{x=r_w} = c_w \frac{dh_w}{dt} \qquad z_1 \le z \le z_2 \tag{14}$$

where c_w is the wellbore storage, $h_w(t)$ is the hydraulic head in the well, and b is the length of the open interval. For an open well test, $c_w = \pi r_c^2$, where r_c is the radius of the well casing, which may be different from the radius of the wellbore r_w. For a pressurized test, $c_w = V_w \gamma_w C_s$, where V_w is the volume of the test section, γ_w is the fluid specific weight, and C_s is the system compressibility [*Neuzil*, 1982; and *Bredehoeft and Papadopulos*, 1980].

By continuity, the hydraulic head in the well $h_w(t)$ is equal to the average head in the formation $h_1(r_w,z,t)$ along the screened portion of the wellbore. Thus

$$h_w(t) = \frac{1}{z_2 - z_1} \int_{z_1}^{z_2} h_1(r_w,z,t)\,dz \qquad t>0 \tag{15}$$

where z_1 and z_2 are the location of the bottom and top of the screen, respectively. Finally, the initial condition for the wellbore is

$$h_w(0) = h_0 + H_0 \tag{16}$$

The above equations can be cast into dimensionless form using the following dimensionless variables.

$$t_D=\frac{K_2 t}{S_{S_2} r_w^2} \qquad \omega=\frac{2S_{S_2} e_2 b r_w}{c_w} \qquad t_s=\omega t_D=\frac{2K_2 e_2 b t}{r_w c_w}$$

$$\alpha=\frac{K_2 e_2}{K_1 e_1} \qquad \gamma=\frac{S_{S_1} e_1}{S_{S_2} e_2} \qquad \beta_1=\frac{K_2 S_{S_3}}{K_{Y_3} S_{S_2}} \qquad \eta=\frac{K_{Y_3} r_w}{K_2 e_2} \qquad \phi=\frac{K_{Z_3}}{K_{Y_3}} \tag{17}$$

$$x_D=\frac{x}{r_w} \qquad z_D=\frac{z}{r_w} \qquad y_D=\frac{y}{r_w} \qquad x_{D_i}=\frac{x_i}{r_w} \qquad z_{D_i}=\frac{z_i}{r_w}$$

$$h_{D_i}=\frac{h_o-h_i}{H_o} \qquad L_D=\frac{L}{r_w} \qquad b_D=\frac{b}{r_w}$$

The solutions for the dimensionless hydraulic head in the wellbore, skin, fracture, and matrix are obtained using the Laplace transform with respect to the dimensionless time t_D, and the finite Fourier transform with respect to the dimensionless spatial variable z_D. The subsidiary equations are solved subject to remaining boundary conditions, and dimensionless solutions in the Laplace domain are obtained by application of the inverse finite Fourier transform. Details of the use of this transform pair are found in *Dougherty and Babu*, [1984]; *Hyder et al.*, [1994]; and *Markle et al.*, [1995].

In the Laplace domain, the dimensionless head in the wellbore is given by

$$\tilde{h}_{D_w}(p)=\frac{\alpha\left[\rho A_1(x_D=1)+\frac{2}{L_D b_D}\sum_{m=1}^{\infty} A_2(x_D=1)A_3^2(\beta_m)\right]}{1+\alpha p\left[\rho A_1(x_D=1)+\frac{2}{L_D b_D}\sum_{m=1}^{\infty} A_2(x_D=1)A_3^2(\beta_m)\right]} \tag{18}$$

where p is the Laplace variable and A_1, A_2, and $A_3(\beta_m)$ are defined by equations (A.1), (A.2), and (A.3) [*Appendix A*]. The other variables are defined in the notation. The solutions to the hydraulic head outside of the wellbore are given in *Markle et al.*, [1997].

Substitution of the solutions into the respective Laplace transformed boundary and continuity conditions verify that the solutions satisfy the boundary and continuity conditions. Also, in the absence of a skin, for a fully penetrating well with an impermeable matrix, equation (18) reduces to the Laplace domain solution given by *Karasaki et al.* [1988]

$$\bar{h}_{D_w}(p) = \frac{1}{\sqrt{\omega p}+p} \tag{19}$$

2.1 Limiting Forms

Limiting forms of equation (18) can be evaluated in the Laplace domain at early and late time using the initial value and final value theorems. The early and late time approximations to equation (18) in the real domain are given in Table 1. These limiting forms provide some insight into the behaviour of the model.

Table 1. Early and Late Time Limiting Forms of $h_{D_w}(t_s)$

	Early Time (small values of ωt_s)		Late Time	
Impermeable Matrix, $h_{D_w}(t_s) \approx$	$1-\frac{2}{\sqrt{\pi}}\sqrt{\frac{\gamma\omega t_s}{\alpha}}$	(20)	$\frac{\rho}{\sqrt{\pi\omega t_s}}$	(21)
Permeable Matrix, $h_{D_w}(t_s) \approx$	$1-\frac{2}{\sqrt{\pi}}\sqrt{\frac{\gamma\omega t_s}{\alpha}}$	(20)	$\frac{1}{\Gamma\left(\frac{1}{4}\right)}\left[\frac{\rho^4\omega^2}{4\eta^2\beta_1(\omega t_s)^3}\right]^{\frac{1}{4}}$	(22)

At early time, a relatively small volume of water has left the wellbore and the test is dominated by the hydraulic properties of media near the wellbore. From equation (20) it is apparent that if a skin is present, this small volume of water is taken up by the compressive storage in the skin and the test is influenced by the hydraulic properties of only the skin. If a skin is not present, the early time response is influenced by the properties of only the fracture and not the matrix. Also, the effects of partial penetration are negligible.

At late time a large volume of water has left the well and the test is dominated by media far from the wellbore. From equation (21) it is apparent that when the matrix is impermeable, the late time response is influenced by the hydraulic properties of only the fracture zone and not the skin zone if one is present. From equation (22) it is apparent that when the matrix is permeable, the late time response is influenced by the hydraulic conductivity of both the fracture and the matrix, as well as the specific storage of the matrix. The specific storage of the fracture does not influence the response. During this time the fracture acts as a planar source/sink of fluid and transient flow occurs only in the matrix. Also, the effects of partial penetration are maximum and the response is equivalent to the fully penetrating case.

3. Results and Discussion

The model presented in the previous section depends on seven dimensionless variables $\gamma/\alpha, x_{D_1}, \omega, \rho, \phi, \beta_1$, and η. Because of the large number of variables, the uniqueness of type curve matching is difficult to assure. The limiting forms of equation (18) are dependent on fewer variables, reducing the uniqueness problem at early and late time. Type curves for these time periods can be developed that are similar to those presented by *Sageev* [1986] who demonstrated the use of three types of plots for radial flow models: log-log early time, semilog intermediate time, and log-log late time. In this section we demonstrate the use of these three plotting methods for the linear flow model (the case where the matrix is impermeable) and for the bilinear flow model (the case where the matrix is permeable) described by equation (18). We discuss the characteristic responses for open well and pressurized slug tests that can be used to distinguish linear and bilinear flow in vertically fractured media from radial flow in unfractured porous media. Also we present criteria defining conditions under which the linear and bilinear flow type curves are unique from radial flow curves given by *Cooper et al.* [1967]. Finally, we discuss the errors that may result from the incorrect interpretation of the test data.

For the general case, type curves are generated by using the *Talbot* [1979] algorithm to numerically invert equation (18). Sensitivity tests indicate that the number of terms required for convergence of the infinite series in equation (18) to a given accuracy, increases for decreasing penetration ratio ρ, and for decreasing values of dimensionless time. In general, stable solutions can be obtained using 50 to 75 terms [*Markle et al.*, 1995]. For solutions involving a fully penetrating well, the summation can be avoided entirely by using simplified forms of equation (18). In the following sections the influence of various combinations of conditions on the response of a slug test are investigated.

3.1 Linear Flow Model - Fully Penetrating Well, Finite Thickness Skin

3.1.1 Early Time Type Curves

Equation (20) indicates that at early time h_{D_w} varies with $(\gamma\omega t_S/\alpha)^{1/2}$. Following the nomenclature adopted by *Sageev* [1986] we will examine the response of

$$h_{D_{w}early} = 1 - h_{D_w} \tag{23}$$

As suggested by equation (20), a log-log plot of $h_{D_{w}early}$ versus $(\gamma\omega t_S/\alpha)^{1/2}$ yields a straight line with unit slope. The effects of a positive skin ($\gamma/\alpha < 1$) and a negative skin ($\gamma/\alpha > 1$) on the early time log-log pressure response for an impermeable matrix are shown in Figure 2 for γ/α ranging from 10^{-10} to 10^{6}. In practice γ/α will rarely be less than 10^{-6}, however the smaller values are shown for completeness. In the absence of a skin ($\gamma/\alpha = 1$) the early response has a unit slope indicating transient linear flow in the fracture.

When a skin is present, the type curves are initially collinear with the curve for no skin. As $\gamma\omega t_S/\alpha$ increases these curves depart from the unit slope. The curves for the positive and negative skin lie above and below the no skin curve respectively. The position of each curve depends on γ/α. After the initial break in slope all responses for negative skins return to a unit slope, where as for positive skins only when $S_T/(\gamma/\alpha) \leq 10^{-3}$ do the responses return to a unit slope. For positive skins with small values of γ/α the curves collapse onto a single curve which has a slope of two.

During the initial period of flow having a unit slope, the head disturbance is limited to the skin zone and the fracture does not influence the response. For a well that is fully

penetrating, the correlating parameter S_T, which is given by

$$S_T=\frac{2S_{S_1}e_1L(x_1-r_w)}{c_w} \tag{24}$$

relates the storage in the skin to the wellbore storage. As the value of S_T increases, the duration of the initial period of flow having a unit slope increases. The departure point from the unit slope response can be collapsed on to a single point on a log-log plot of $h_{D_w early}/S_T$ versus $(\gamma\omega t_S/\alpha)^{1/2}/S_T$ as shown in Figure 2 for S_T ranging from 10^{-2} to 10^{-10}. As shown, the break in slope occurs when $(\gamma\omega t_S/\alpha)^{1/2}/S_T = 1$ and $h_{D_w early}/S_T = 1$. From these expressions the time of the break is given by

$$t=\frac{S_{S_1}}{K_1}(x_1-r_w)^2 \tag{25}$$

and the dimensionless head in the well is given by $h_{D_w} = 1\text{-}S_T$. For values of $S_T < 10^{-2}$ the break will occur at less than 1% decay in the initial head. In these cases the observation of the first linear portion of the response is unlikely. For values of $S_T > 10^0$ the break will not occur since the skin dominates the response for the entire duration of the test.

Consideration of practical ranges in values indicates that for open well tests the range of ω is $10^{-11} \leq \omega \leq 10^{-7}$ and the corresponding range of S_T is $10^{-13} \leq S_T \leq 10^0$. Therefore in a large portion of this range one may not observe the initial period of linear flow during an open well test. For pressurized tests the wellbore storage, c_w, maybe between four and seven orders of magnitude smaller than for open well tests. As a result the ranges of ω and S_T are $10^{-6} \leq \omega \leq 10^{-2}$ and $10^{-8} \leq S_T \leq 10^5$. Therefore for a pressurized test the skin is more likely to dominate the entire response. This suggests that the testing method plays a significant role in determining which portion of the response will be observed and which conditions will influence the response.

From equation (25), if $K_1 = 10^{-6}$ m/s, $S_{S_1} = 10^{-4}$ m^{-1}, $x_1 = 0.5$ m, and $r_w = 0.01$ m the break will occur 24 s into the test. If $K_1 = 10^{-5}$ then the break occurs after 2.4 s. In these cases the observation of the initial, linear flow response will depend upon the ability to rapidly measure small changes in head in the well. A practical range in values for S_{S_1}/K_1 is 10^{-6} to 10^{7} s/m^2 and for x_1-r_w is 10^{-3} to 10 m, which gives times ranging from 10^{-12} to 10^{9} s. In approximately 60 percent of this range the break occurs within the first second of the test and in 15 percent the break occurs after 24 hours. During a slug test, generally good quality, early time data is not obtained within the first few seconds of the test, and usually the test is stopped within 24 hours. Thus, the detection of a skin with the early time plot will be possible in about 25 percent of the practical range in values. Given good quality data, a match to early time type curves provides an estimate of S_T, γ/α, $K_1 S_{S_1} e_1^2$ and $K_2 S_{S_2} e_2^2$. Data from the initial period of linear flow and equation (20) also provides an estimate $K_1 S_{S_1} e_1^2$.

For radial flow tests, the unit slope and the subsequent increase in slope is a characteristic log-log early time response for both the no skin and finite skin cases. However, once the initial break from unit slope occurs the response does not return to the unit slope. Tests indicate that provided $S_T/(\gamma/\alpha) \leq 10^{-3}$ the type curves for linear flow are distinct from type curves for radial flow. For open well tests this criterion will rarely be satisfied and the early time response does not provide a method to uniquely distinguish linear flow in a vertical fracture from radial flow. Under some test conditions the criterion may be satisfied for pressurized tests.

3.1.2 Intermediate Time Type Curves

The effect of a skin on the semilog response is shown in Figure 3 for $S_T = 10^{-4}$, $\rho = 1$ and γ/α ranging from 10^{-1} to 10^{-5}. Here h_{D_w} is plotted versus $\omega t_S/\rho^2$. The semilog response for the no skin case ($\gamma/\alpha = 1$) [*Karasaki et al.*, 1988], is included for comparison. A positive skin shifts the type curve to larger ωt_S and steepens the slope. As the value of γ/α decreases the

effect of the skin increases. In contrast, the effect of a negative skin is negligible and a negative skin will never be detected. Not shown in Figure 3 are the type curves for $\gamma/\alpha < 10^{-5}$. For very small values of γ/α the type curves shift to larger values of ωt_S, the shape of the curves become identical, and a unique match cannot be obtained. Interpretation under these conditions will yield correct estimates of the properties of only the skin $K_1 S_{S_1} e_1^2$.

Karasaki et al. [1988] showed that the semilog type curve for linear flow has a much gentler slope or longer response time than type curves for radial flow. This longer response on a semilog plot is diagnostic of linear flow. However, comparison of Figure 3 with *Cooper et al.* [1967] curves indicates that there are only subtle differences between the type curves for linear flow with small values of γ/α and large values of S_T, and curves for radial flow with small dimensionless wellbore storage coefficients ($C_D < 10^{-4}$). Provided $S_T/(\gamma/\alpha) \leq 10$, the semilog type curves for linear flow are distinct from type curves for radial flow. Field conditions exist which fall on either side of this criterion for both open and pressurized tests. Thus, if a positive skin is present, distinguishing linear flow from radial flow with the semilog plot may not be possible under all conditions. For example, consider an open well test where $r_w = 0.01$ m, $r_c = 0.01$ m, $L = 2$ m, $x_1 = 1.68$ m, $K_1 = 10^{-6}$ m/s, $K_2 = 1$ m/s, $S_{S_1} = 4\times10^{-5}$ m^{-1}, $S_{S_2} = 4\times10^{-6}$ m^{-1}, and $e_1 = e_2$. In this example $S_T/(\gamma/\alpha) = 10^2$. Interpretation of the simulated response using the *Cooper et al.* [1967] solution yields a hydraulic conductivity of 1.6×10^{-9} m/s and a specific storage of 5×10^{-7} m^{-1}. Not only is the presence of the highly conductive fracture, which may significantly influence the transport of contaminants, undetected, but also radial flow conditions are mistakenly assumed.

3.1.3 Late Time Type Curves

Figure 4 presents the effect of a skin on the late time log-log response for $S_T = 10^{-4}$, $\rho = 1$ and γ/α ranging from 10^{-5} to $\geq 10^{-2}$. Here h_{D_w} is plotted versus $(\omega t_S/\rho^2)^{1/2}$ as suggested by

equation (21). A positive skin influences the early portion of the response. At late time all curves merge from above with the no skin curve having a unit negative slope, indicative of transient linear flow at late time. A negative skin has no apparent influence the response. In general the late time response depends on only the fracture properties as indicated by equation (21).

As S_T increases and γ/α decreases the influence of the skin on the late time response increases. During most slug tests, values of h_{D_w} are not measured below 10^{-3}. For tests influenced by a positive skin with a large S_T and small γ/α (ie. many pressurized tests), the skin may have a significant effect on the late time data. Under these conditions the linear portion of the late time response may not be observed and linear flow may not be detected. However, provided the unit negative slope is observed during the test, a match to the late time type curves provides an estimate of S_T and γ/α. The linear portion of the data and equation (21) provides an estimate of the fracture property $K_2 S_{S_2} e_2^2$.

For radial flow, a log-log plot of h_{D_w} versus $(t_D/C_D)^{1/2}$ yields a linear response having a slope of -2 in the absence of a skin. When a positive skin is present, the late time type curves merge from above with the no skin curve having a slope of -2. Therefore, a slope of -1 on the late time log-log plot uniquely distinguishes linear flow from radial flow.

3.2 Bilinear Flow Model - Fully Penetrating Well, No Skin

3.2.1 Early Time Type Curves

The effect of matrix flow on the early time log-log response is shown in Figure 5. The well is fully penetrating and no skin is present. Initially all of the responses follow the linear flow type curve (impermeable matrix, $\Delta=0$) and then depart forming a family of bilinear flow curves (permeable matrix, $\Delta > 0$) above the linear flow curve. The departure point and final

separation are controlled by the correlating parameter Δ, where

$$\Delta = \frac{\eta}{\omega}\sqrt{\beta_1} \tag{25}$$

which relates the dimensionless wellbore storage to the hydraulic properties of the matrix and fracture. As Δ increases the effect of matrix flow increases due to a quicker build up of wellbore pressure. A match of the early time data provides an estimate of $K_2 S_{S_2} e_2^2$ and Δ. Provided the response during the linear flow period is measured, equation (20) may be used to estimate $K_2 S_{S_2} e_2^2$.

For $\Delta > 1$ the influence of matrix flow is significant at early time. The break from linear flow occurs within the first few seconds of the test when head changes in the well are very small. Therefore the linear flow portion of the response may not be observed. For $\Delta \leq 1.0$ the influence of matrix flow is negligible and the impermeable matrix assumption is valid at early time. The practical ranges in Δ for open well and pressurized tests are $1 \leq \Delta \leq 10^{11}$ and $10^{-4} \leq \Delta \leq 10^{6}$, respectively. This suggests that in general at early time the influence of matrix flow is significant during open well tests, while it may be insignificant during many pressurized tests. Thus the each test method may be used to target specific conditions that may influence a test. For example, within a given test interval or well one can minimize the influence of the matrix flow by conducting a pressurized test, and subsequently minimize the influence of a skin by conducting an open well test.

The type curves for bilinear flow, shown in Figure 5 are similar to the curves for linear flow with of a positive skin as well as curves for radial flow. Therefore, some non-uniqueness can result at early time between linear, bilinear, and radial flow using the log-log plot of early time data.

3.2.2 Intermediate Time Type Curves

The effect of matrix flow on the semilog response is shown in Figure 6 for $\rho = 1$, and Δ ranging from 0 to 10^2. As Δ increases and the influence of matrix flow increases, the type curves shift to smaller $\omega t_s/\rho^2$ and the slope becomes steeper. For values of $\Delta > 1$ the shape of type curves is similar and a unique match cannot be obtained. For values of $\Delta \leq 10^{-2}$ the effect of matrix flow is negligible. In practice, this criterion will only be satisfied for some pressurized tests, suggesting that the influence of matrix permeability on the intermediate time data must always be considered for open well tests. This imposes a significant restriction on the use of the linear flow model for open well tests.

Comparison of Figure 6 with Figure 3 indicates that for $\Delta > 1$, the type curves for bilinear flow are similar to those for linear flow with a positive skin and small γ/α. Similarly, for $\Delta > 1$ it is difficult to distinguish between semilog type curves for bilinear flow, and curves for radial flow with large dimensionless wellbore storage coefficients ($C_D \approx 10^{-1}$). This is expected since as flow progresses from linear to bilinear it increasingly approximates a radial flow system. Thus, when the influence of matrix flow is significant ($\Delta > 1$), distinguishing bilinear flow from either linear fracture flow influenced by a positive skin or radial flow will not be possible with the semilog plot.

The error that may result from interpreting a test influenced by bilinear flow with the radial flow model is shown in the following example. Consider a system where $K_2 = 1$ m/s, $K_3 = 2\times10^{-9}$ m/s, $S_{S_2} = 4\times10^{-6}$ m^{-1}, $S_{S_3} = 10^{-7}$ m^{-1}, $L = 2$ m, $r_w = 0.01$ m and $r_c = 0.01$ m, then $\Delta = 10^2$. Interpretation of the simulated response using the *Cooper et al.* [1967] solution yields a hydraulic conductivity of 1.3×10^{-6} m/s and a specific storage of 2×10^{-2} m^{-1}. This interpretation does not account for the presence of the fracture, and the estimated hydraulic conductivity for the matrix is three orders of magnitude larger than the actual hydraulic

conductivity.

3.2.3 Late Time Type Curves

The effect of matrix flow on the late time log-log response is shown in Figure 7. A log-log plot of h_{D_w} versus $(\omega t_S/\rho^2)^{1/2}$ produces a linear response having a slope of -1.5. Equation (22) indicates that the late time response is not influenced by the presence of a skin, and that steady state flow occurs in the fracture which acts as a planar source/sink. Transient flow occurs in only the matrix. As shown in Figure 7, as Δ increases steady state flow in the fracture begins at smaller values of $(\omega t_S/\rho^2)^{1/2}$. For $\Delta > 1$ the type curves are similar in shape. Type curve matches in this region will be nonunique. For $\Delta < 10^{-1}$, the late time response is initially collinear with the linear flow curve. As $(\omega t_S/\rho^2)^{1/2}$ increases the curves deviate below the unit negative slope forming a family of curves having a slope of -1.5. Provided the late time slope of -1.5 is attained during a test, a match of the data provides an estimate of Δ. If the late time response also includes a unit negative slope response, an estimate of $K_2 S_{S_2} e_2^2$ may be determined with equation (21).

From Figure 7 it is apparent that at late time, provided $\Delta \leq 10^{-3}$ the effect of matrix flow is negligible. This condition will rarely be satisfied for either open well or pressurized tests, and the influence of matrix flow must always be considered at late time.

The log-log plot of late time data has a slope of -2 for radial flow, -1.5 for bilinear flow, and -1 for linear flow. Therefore the log-log plot of late time data may be used to uniquely identify tests influenced by bilinear, or linear flow from tests conducted under conditions of radial flow.

3.3 Bilinear Flow Model - Fully Penetrating Wellbore, Finite Thickness Skin

3.3.1 Early Time Type Curves

Figure 8 shows the combined effects of a skin and a permeable matrix on the early time log-log response for $S_T = 10^{-4}$ to 10^{-10}, $\rho = 1$, $\Delta = 10$ and γ/α ranging from 10^{6} to 10^{-10}. As shown in Figure 8, all the curves depart at the same point as in the linear flow case with the exception of the family of curves for $S_T = 10^{-4}$. For linear flow, the break from the unit slope response occurs when flow between the skin and the fracture begins, while for bilinear flow, the break occurs when the effect of matrix flow becomes significant. When both a permeable matrix and a skin having a small S_T are present, the effect of the fracture may influence the response before the effect of matrix flow becomes significant. Under these conditions all curves will depart at one point which is dependent upon S_T as in the case of linear flow. If S_T or Δ are large, the effect of matrix flow may influence the response before the effect of the fracture becomes significant. Under these conditions, the departure point for each curve will depend upon Δ, and S_T will not be a correlating parameter.

In general, provided the early time criterion established for bilinear flow without a skin ($\Delta \leq 1$) is satisfied, the impermeable matrix assumption is valid even when a skin is present. Under these conditions the linear flow type curves can be used. However, when $\Delta > 1$ the influence of matrix flow on the early time response is significant and the effect of matrix flow must be considered.

Comparison of Figure 8 to Figure 2 for linear flow with a skin, and to Figure 5 for the bilinear flow without a skin indicates that similar responses were obtained. Therefore the early time response suffers problems of uniqueness. Similarly, the early time response can not be used to distinguish bilinear flow influenced by a skin from radial flow.

3.3.2 Intermediate Time Type Curves

The intermediate time semilog responses are not shown but were found to be similar to the responses for linear flow with a skin, bilinear flow without a skin, and radial flow. Therefore, the intermediate time plot has severe problems of uniqueness and can not be used to identify the various conditions that may be influencing the test data. Also, results indicate that the interpretation of tests influenced by both bilinear flow and a skin using radial flow methods may yield large errors. Not only is the presence of the fracture missed, but also errors of up to five orders of magnitude in the estimate of the matrix hydraulic conductivity can occur. This suggests that if the presence vertical fractures is suspected, the semilog type curves should never be the sole method used to interpret the results from a slug test.

3.3.3 Late Time Type Curves

Figure 9 is the late time log-log response for $\Delta = 10$, $S_T = 10^{-4}$ and $\gamma/\alpha = \leq 1$ to 10^{-5}. As in the case of linear flow, the early portion of the response is influenced by the presence of a positive skin while a negative skin does not influence the response. At late time all curves merge with the no skin, permeable matrix curve with a slope of -1.5. Therefore, even when a skin is present the late time log-log plot may be used to identify tests influenced by bilinear flow provided the late time slope of -1.5 is measured during the test.

3.4 Partial Penetration

Results indicate that the effect of partial penetration on the response is similar to the effect of a skin and of a permeable matrix. It is not possible to uniquely identify tests influenced by partial penetration using any of the three plotting methods. Therefore it is important either to minimize the effects of partial penetration through well and test design, or to incorporate it's influence into the interpretation of the test data. The influence of partial penetration can be minimized by maximizing the length of the screened interval or the test section. Also, to

properly account for the effect of partial penetration in the interpretation of the data, the collection of high quality geological data during well construction and installation is a necessity.

3.5 Anisotropic Matrix

The effect of matrix anisotropy was found to be negligible. In comparison to the vertical flow in the matrix, flow in the fracture is the dominant mechanism for the movement of fluid vertically within the system. The rapid vertical flow in the fracture results in a planar source/sink at the fracture-matrix interface. As a result, flow in the matrix is essentially one dimensional normal to the plane of the fracture.

4. Conclusions

A new semi-analytical model incorporating bilinear flow theory was presented for the slug test. The model can be used in the interpretation of open well and pressurized slug tests conducted in vertically fractured formations. The model accounts for the presence of a matrix with a moderate to low permeability and a skin having a finite thickness. The model is particularly useful where it is known that a vertical fracture intersects the wellbore. For these cases the model can be used to generate type curves for early, intermediate, and late time. Using the curves and the limiting equations conditions that influenced the test, such as the presence of a skin or matrix flow, can be assessed and the hydraulic properties of the fracture, skin and matrix can be estimated.

The influence on the early time log-log plot of a positive skin or matrix flow are similar and represented by an upward deviation from the initial period of linear flow having a unit slope. In general the influence of a skin is more significant on the pressurized test while the influence of matrix flow is more significant during open well tests. Therefore the test method

can be selected to minimize or maximize the influence of one condition over another. Under some conditions the early time responses for linear and bilinear flow are similar to the response for radial flow and some non-uniqueness results.

A gentle slope and long response on the semilog plot of intermediate time data has previously been shown to be diagnostic of linear fracture flow. The effects of either a positive skin or a permeable matrix are to steepen the slope and shorten the response. Some non-uniqueness exists and it may be difficult to identify which of these factors has influenced the test. Of particular importance is the influence of a skin or matrix flow, which if significant, the semilog responses may be mistaken for tests conducted in conditions of radial flow. Interpretation of the test data using the radial flow models not only fails to account for the presence of the fracture, but also may yield estimates of the hydraulic parameters for the matrix that are in error by several orders of magnitude. Therefore where the potential for vertical fractures exists the semilog plot should never be the sole method of analysis.

At late time, in general the influence of a skin is not significant for open well or pressurized tests, while the influence of matrix flow is significant for all open well and many pressurized tests. As a result, the late time data will demonstrate characteristic responses diagnostic of linear flow, slope of -1, and bilinear flow, slope of -1.5. These responses are unique from the responses for radial flow which have a slope of -2 at late time. Thus, the late time plot provides the best method to for distinguishing between linear, bilinear and radial flow. To ensure that these characteristic responses are obtained it is critical that small head changes late in the test be measured.

In general, the presence of a skin complicates the interpretation of the test data. The influence of the skin can make it difficult to distinguish between linear, bilinear, or radial flow

responses. Therefore, to maximize the probability of identifying linear or bilinear flow it is important to minimize the formation of a skin. This may be facilitated by selecting appropriate drilling, well installation and development methods. Also the influence of the skin can be minimized by conducting an open well test or maximized by conducting a pressurized test. In addition, the careful collection of good quality geological information may indicate the presence of vertical fractures thereby assisting one in properly interpreting test results.

Appendix A

$$A_1(x_D)=\frac{1}{q_1'}\left[\frac{\exp[(1-x_D)q_1']-\xi'\exp[(1-2x_{D_1}+x_D)q_1']}{1+\xi'\exp[2(1-x_{D_1})q_1']}\right] \tag{A.1}$$

$$A_2(x_D)=\frac{1}{q_1}\left[\frac{\exp[(1-x_D)q_1]-\xi\exp[(1-2x_{D_1}+x_D)q_1]}{1+\xi\exp[2(1-x_{D_1})q_1]}\right] \tag{A.2}$$

$$A_3(\beta_m)=\frac{1}{\beta_m}[\sin(\beta_m z_{D_2})-\sin(\beta_m z_{D_1})] \tag{A.3}$$

Notation

A_1	group defined by equation (A.1)
A_2	group defined by equation (A:2)
$A_3(\beta_m)$	group defined by equation (A.3)
b	screen length, L
b_D	dimensionless screen length
C_s	system compressibility, LT^2M^{-1}
c_w	wellbore storage coefficient, L^2
e_i	fracture aperture in i, L
h_i	hydraulic head in i, L

h_{D_i}	dimensionless hydraulic head in i
$h_{D_{w early}}$	early time dimensionless hydraulic head in wellbore
h_o	initial head outside of the wellbore, L
H_o	initial head in wellbore, L
K_i	hydraulic conductivity in i, L^2T^{-1}
K_{Y_3}	horizontal hydraulic conductivity in matrix, L^2T^{-1}
K_{Z_3}	vertical hydraulic conductivity in matrix, L^2T^{-1}
L	fracture height, L
L_D	dimensionless fracture height
m	Fourier transform variable
p	Laplace transform variable
q_1	$\sqrt{2\alpha\eta q_3+\alpha\gamma\omega p+\beta_m^2}$
q_1'	$\sqrt{2\alpha\eta q_3'+\alpha\gamma\omega p}$
q_2	$\sqrt{2\eta q_3+\omega p+\beta_m^2}$
q_2'	$\sqrt{2\eta q_3'+\omega p}$
q_3	$\sqrt{\omega\beta_1 p+\phi\beta_m^2}$
q_3'	$\sqrt{\omega\beta_1 p}$
r_c	wellbore casing radius, L
r_w	wellbore radius, L

S_{S_i}	specific storage in i, L^{-1}
S_T	storage ratio
t	time, T
t_D	dimensionless time, $\frac{K_2 t}{S_{S_2} r_w^2}$
t_s	dimensionless group, ωt_D
x	horizontal coordinate, L
x_D	dimensionless horizontal coordinate
x_1	horizontal coordinate of the outer boundary of the skin, L
x_{D_1}	dimensionless coordinate of the outer boundary of the skin
V_w	volume of the test section, L^3
y	lateral coordinate in matrix, L
y_D	dimensionless lateral coordinate in matrix
z	vertical coordinate, L
z_D	dimensionless vertical coordinate
z_1	lower z coordinate of well screen, L
z_{D_1}	dimensionless bottom of well screen
z_2	upper z coordinate of well screen, L
z_{D_2}	dimensionless top of well screen
α	transmissivity ratio, $K_2 e_2 / K_1 e_1$

γ	storativity ratio, $S_{S_1} e_1 / S_{S_2} e_2$
γ_w	specific weight of fluid, $ML^{-2}T^{-2}$
β_m	eigenvalue for finite Fourier transform, $\frac{m\pi}{L_D}$
β_1	$\frac{K_2 S_{S_3}}{K_{Y_3} S_{S_2}}$
η	$\frac{K_{Y_3} r_w}{K_2 e_2}$
ρ	partial penetration ratio, b/L
λ	$q_1/(\alpha q_2)$
λ'	$q_1'/(\alpha q_2')$
ξ	$(1-\lambda)/(1+\lambda)$
ξ'	$(1-\lambda')/(1+\lambda')$
ϕ	matrix anisotropy ratio, K_{Z_3}/K_{Y_3}
ω	dimensionless wellbore storage coefficient, $\frac{2 S_{S_2} e_2 b r_w}{c_w}$
Δ	correlating parameter, $\frac{\eta}{\omega}\sqrt{\beta_1}$
$\Gamma\left(\frac{1}{4}\right)$	gamma function

Other

$\tilde{h}$	Laplace transform of h

Subscripts

D	dimensionless
1	region 1, skin
2	region 2, fracture
3	region 3, matrix
w	wellbore

Acknowledgment. This work was supported by Environment Canada

References

Barker, J. A., and J. H. Black, Slug tests in fissured aquifers, *Water Resour. Res.*, *19*(6), 1558-1564, 1983.

Bredehoeft, J. D., and S. S. Papadopulos, A method for determining the hydraulic properties of tight formations, *Water Resour. Res.*, *16*(1), 233-238, 1980.

Cinco-Ley, H., F. Samaniego-V, and N. A. Dominquez, Transient pressure behaviour for a well with a finite-conductivity vertical fracture, *Soc. Pet. Eng. J.*, 253-264, 1978.

Cinco-Ley, H., and F. Samaniego-V, Transient pressure analysis for fractured wells, *J. Pet. Technol.*, *33*, 1749-1766, 1981.

Cooper, H. H., J. D. Bredehoeft, and S. S. Papadopulos, Response of a finite diameter well to an instantaneous charge of water, *Water Resour. Res.*, *3*(1), 263-269, 1967.

D'Astous, A. Y., W. W. Ruland, J. R. G. Bruce, J. A. Cherry, and R. W. Gillham, Fracture effects in the shallow groundwater zone in weathered Sarnia-area clay, *Can. Geotech. J.*, *26*, 43-56, 1988.

Dougherty, D. E., and D. K. Babu, Flow to a partially penetrating well in a double-porosity reservoir, *Water Resour. Res.*, *20*(8), 1116-1122, 1984.

Grader, A. S., and H. J. Ramey, Jr., Slug-test analysis in double-porosity reservoirs, *Soc. Pet. Eng. Form. Eval.*, 329-339, June 1988.

Gringarten, A. C., H. J. Ramey, Jr., and R. Raghavan, Unsteady-state pressure distributions created by a well with a single infinite-conductivity vertical fracture, *Soc. Pet. Eng. J. (14)*4, 347-360, *AIME. 257*, 1974.

Grisak, G. E., and J. A. Cherry, Hydrologic characteristics and response of fractured till and clay confining a shallow aquifer, *Can. Geotech. J., 12*, 23-43, 1975.

Hinsby, K., L.D. McKay, P. Jõrgensen, M. Lenczewski, and C.P. Gerba, Fracture Aperture Measurements and Migration of Solutes, Viruses, and Immiscible Creosote in a Column of Clay-Rich Till, *Ground Water, 33*(6), 1065-____, 1996.

Hyder, Z., J. J. Butler, Jr., C. D. McElwee, and W. Liu, Slug tests in partially penetrating wells, *Water Resour. Res., 30*(11), 2945-2957, 1994.

Karasaki, K., J. C. S. Long, and P. A. Witherspoon, Analytical models of slug tests, *Water Resour. Res., 24*(1), 115-126, 1988.

Keller, C. K., G. van der Kamp, and J. A. Cherry, Fracture permeability and groundwater flow in clayey till near Saskatoon, Saskatchewan, *Can. Geotech. J., 23*, 229-240, 1986.

Kissling, W., and R. M. Young, Two-dimensional flow in a fractured medium, *Transport in Porous Media, 4*, 335-368, 1989.

Markle, J. M., K. S. Novakowski, and R. K. Rowe, A model for the constant-head pumping test conducted in vertically fractured media, *Int. J. Numer. Anal. Methods Geomech., 19*, 457-473, 1995.

Markle, J. M., K. S. Novakowski, and R. K. Rowe, A model for slug tests conducted in vertically fractured media, *Geotechnical Rep. #GEO_____*, __ pp., University of Western Ontario, London, 1997.

McKay, D. L., J. A. Cherry, and R. W. Gillham, Field experiments in fractured clay till 1. Hydraulic conductivity and fracture aperture, *Water Resour. Res.*, *29*(4), 1149-1162, 1993.

Moench, A. F., and P. A. Hsieh, Analysis of slug test data in a well with finite thickness skin, paper presented at the I.A.H. 17th International Congress on Hydrology of rocks of low permeability, Int. Assoc. Hydrogeol., Tucson, AZ., Jan. 7-12, 1985.

Neuzil, C. E., and J. V. Tracy, Flow through fractures, *Water Resour. Res.*, *17*(1), 191-199, 1981.

Neuzil, C. E., On conducting the modified 'slug' test in tight formations, *Water Resour. Res.*, *18*(2), 439-441, 1982.

Prats, M., The effect of vertical fractures on reservior behavior-incompressible fluid case, *SPEJ*, 105-118, 1962.

Raven, K. J., Hydraulic characterization of a small ground-water flow system in fractured monzonitic gneiss, National Hydrological Research Institute, Paper No. 30, Inland Water Directorate, Ottawa Canada, p. 133, 1986.

Roberts, J. R., J. A. Cherry, and F. W. Schwartz, A case study of a chemical spill: polychlorinated biphenyls (PCBs) 1. History, distribution, and surface translocation, *Water Resour. Res.*, *18*(3), 525-534, 1982.

Rudolph, D. L., J. A. Cherry, and R. N. Farvolden, Groundwater flow and solute transport in fractured lacustrine clay near Mexico City, *Water Resour. Res.*, *27*(9), 2187-2201, 1991.

Sageev, A., Slug test analysis, *Water Resour. Res.*, *22*(8), 1323-1333, 1986.

Sudicky, E. A., and R. G. McLaren, The Laplace transform Galerkin technique for large-scale simulation of mass transport in discretely fractured porous formations, *Water Resour. Res.*, *28*(2), 499-514, 1992.

Talbot, A., The accurate numerical inversion of Laplace transforms, *J. Inst. Applic.*, *23*, 97-120, 1979.

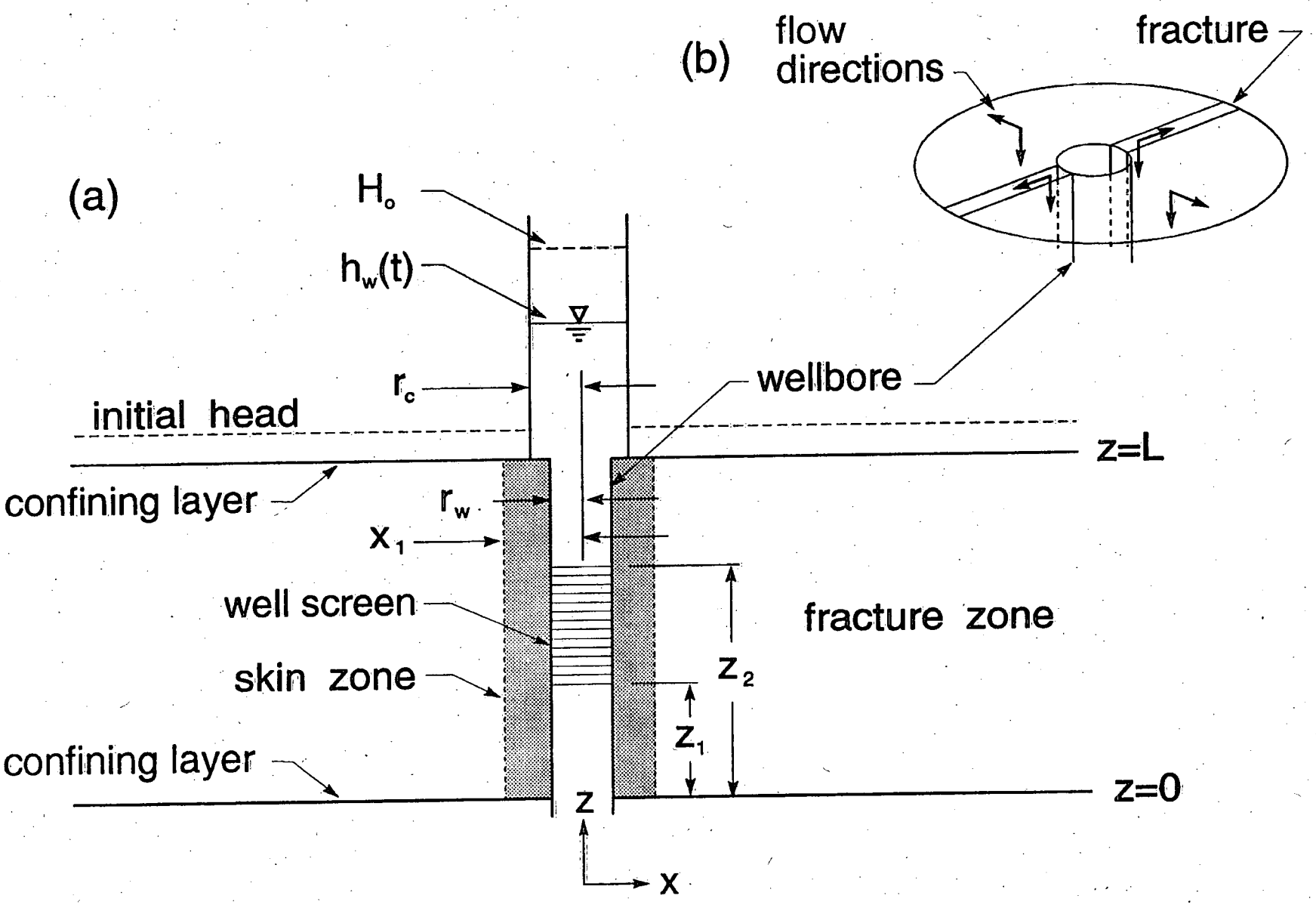

Figure 1. Schematic diagram showing (a) an open-well slug test conducted in a partially penetrating well surrounded by a finite-thickness skin, and (b) flow directions in the vertical fracture and matrix. For a pressurized slug test, packers would be used to isolate the test section.

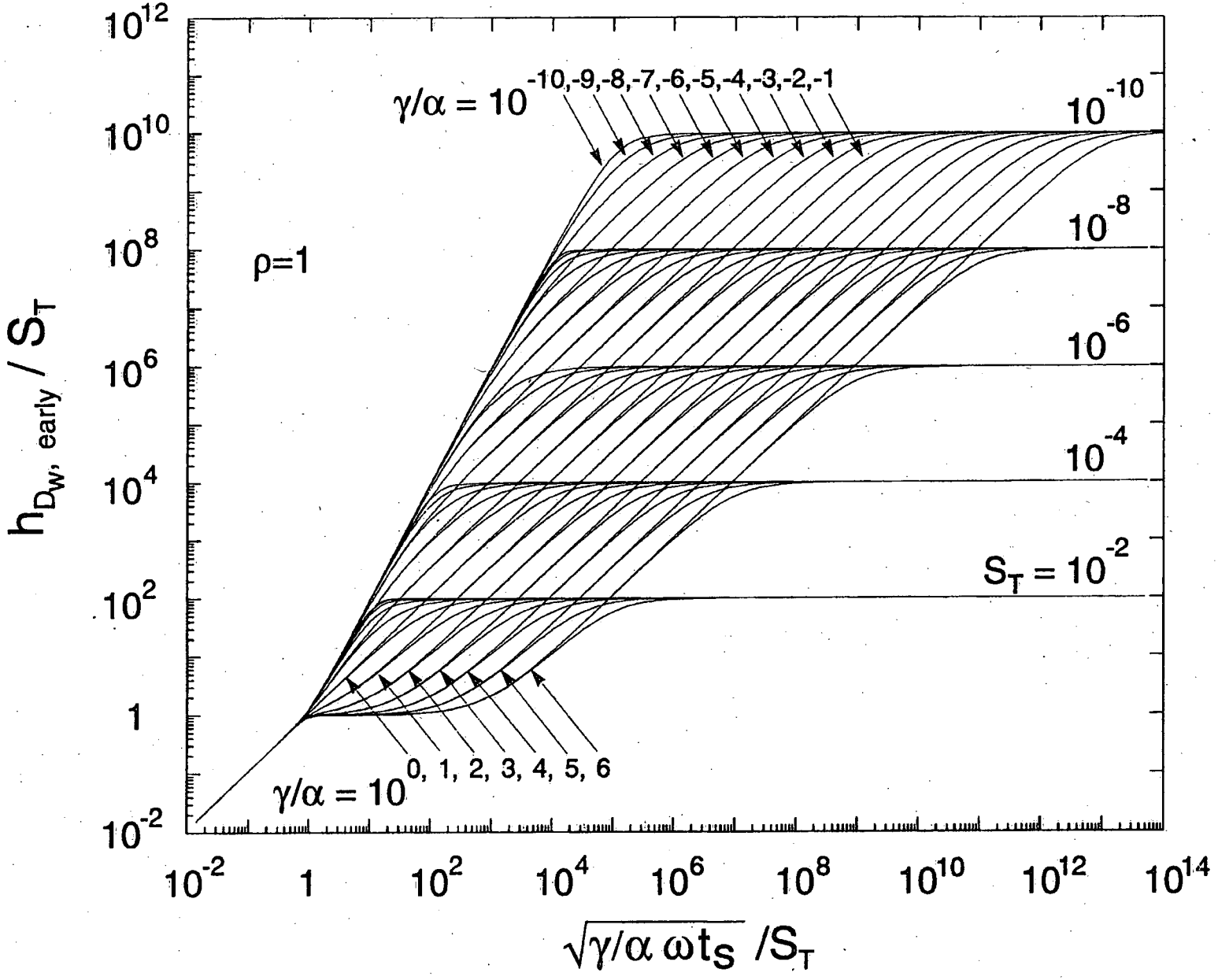

Figure 2. Log-log type curves for the early time response (normalized by $1/S_T$) of a slug test in a fully penetrating wellbore having a finite thickness skin and an impermeable matrix. Curves are shown for γ/α ranging from 10^{-10} to 10^{6} (left to right), S_T ranging from 10^{-10} to 10^{-2} (top to bottom), and ρ equal to 1.0.

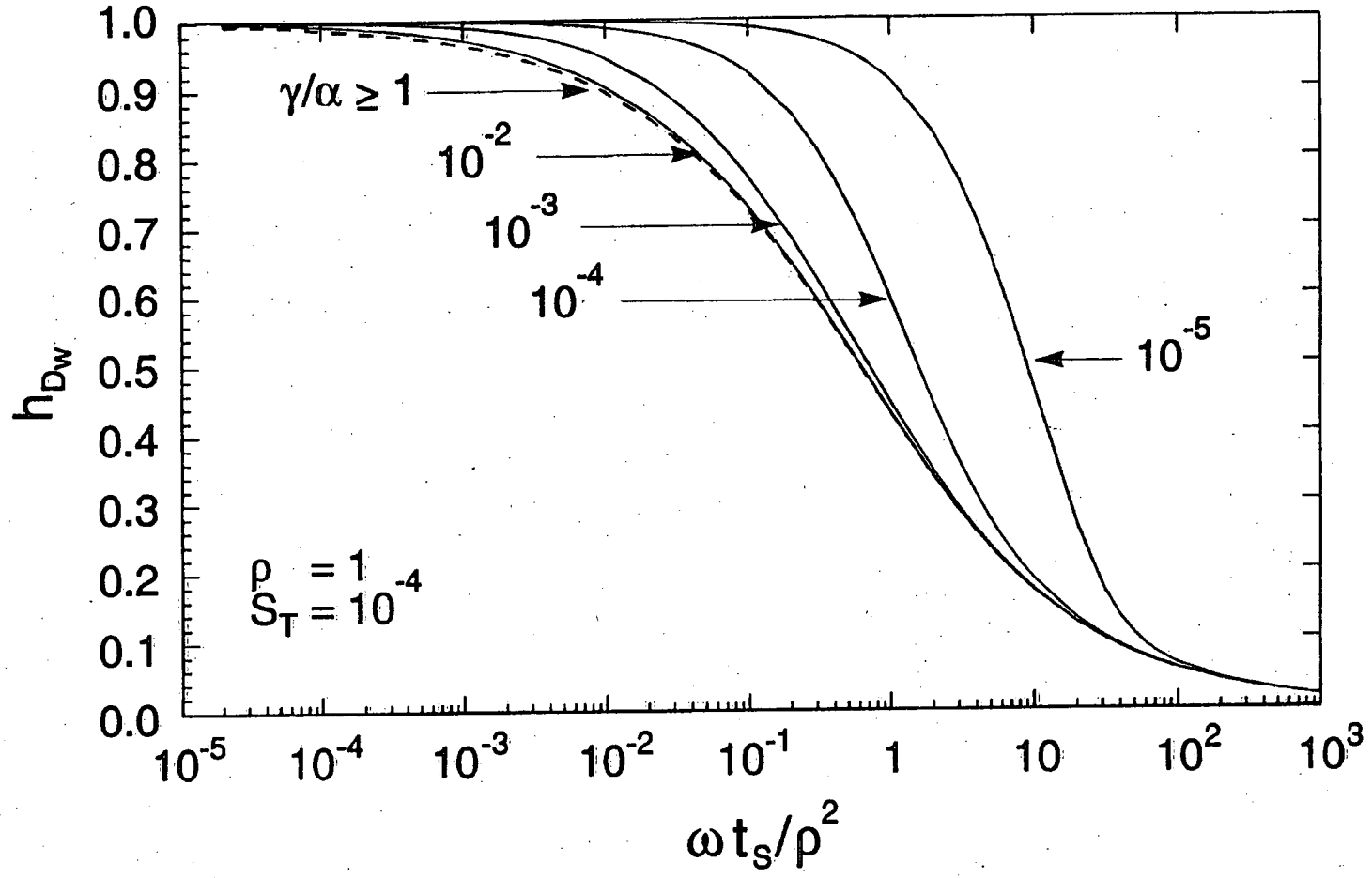

Figure 3. Intermediate time semilog type curves for a slug test in a fully penetrating wellbore with a finite thickness skin and an impermeable matrix. Curves are shown for γ/α ranging from 10^{-5} to ≥ 1 (right to left), S_T equal to 10^{-4}, and ρ equal to 1.0.

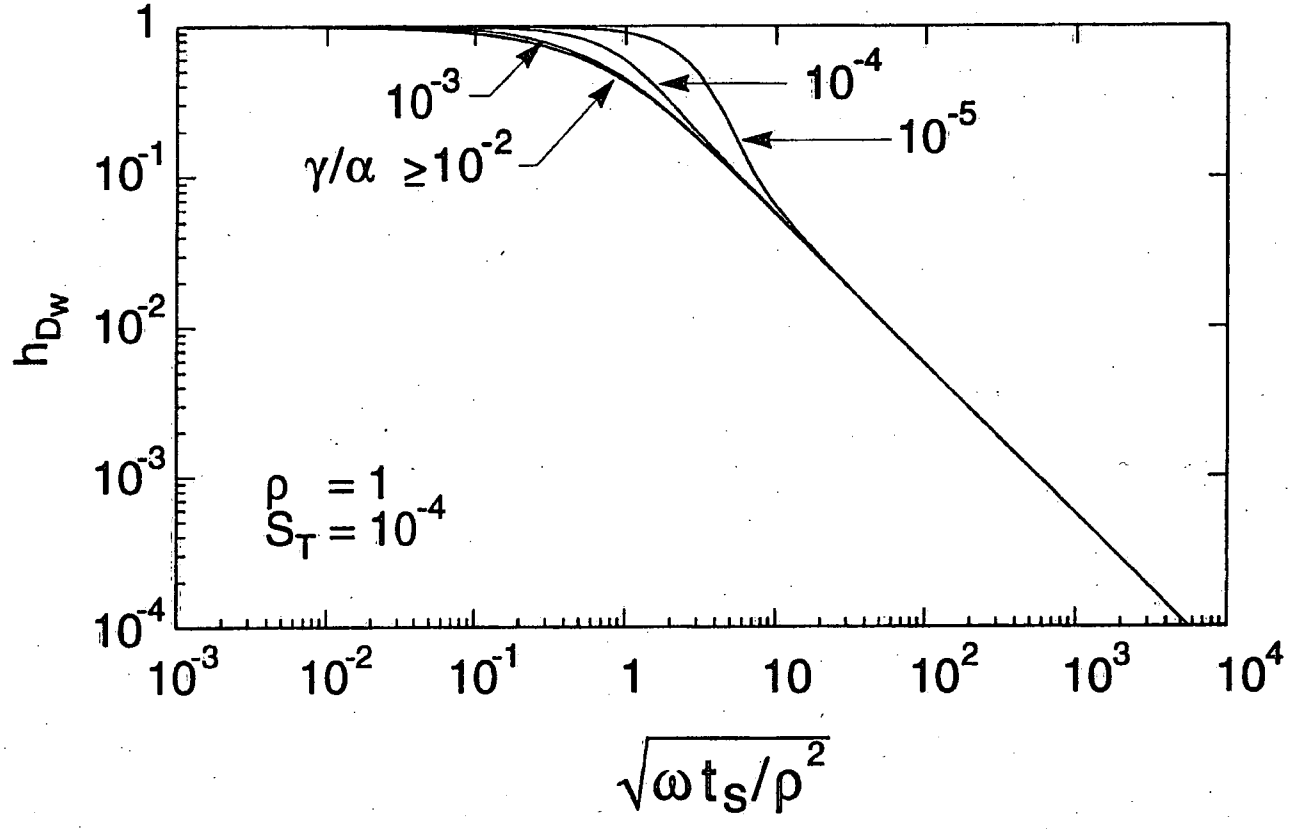

Figure 4. Log-log type curves for the late time response of a slug test in a fully penetrating wellbore having a finite thickness skin and an impermeable matrix. Curves are shown for γ/α ranging from 10^{-5} to $\geq 10^{-2}$ (right to left), S_T equal to 10^{-4}, and ρ equal to 1.0.

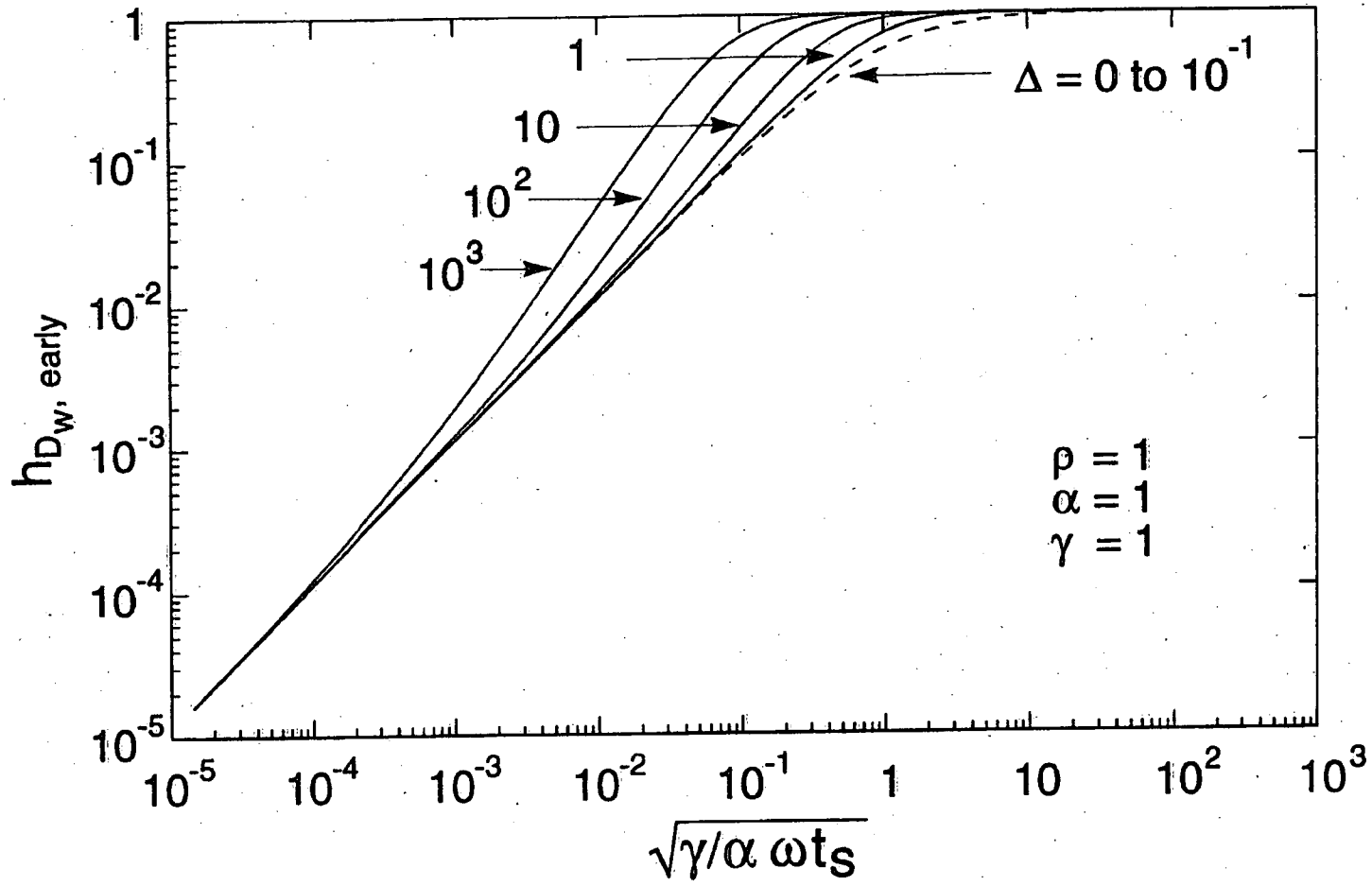

Figure 5. Log-log type curves for the early time response of a slug test in a fully penetrating wellbore with a permeable matrix. No skin is present (α and γ equal 1.0), Δ ranges from 0 to 10^3, and ρ equals 1.0.

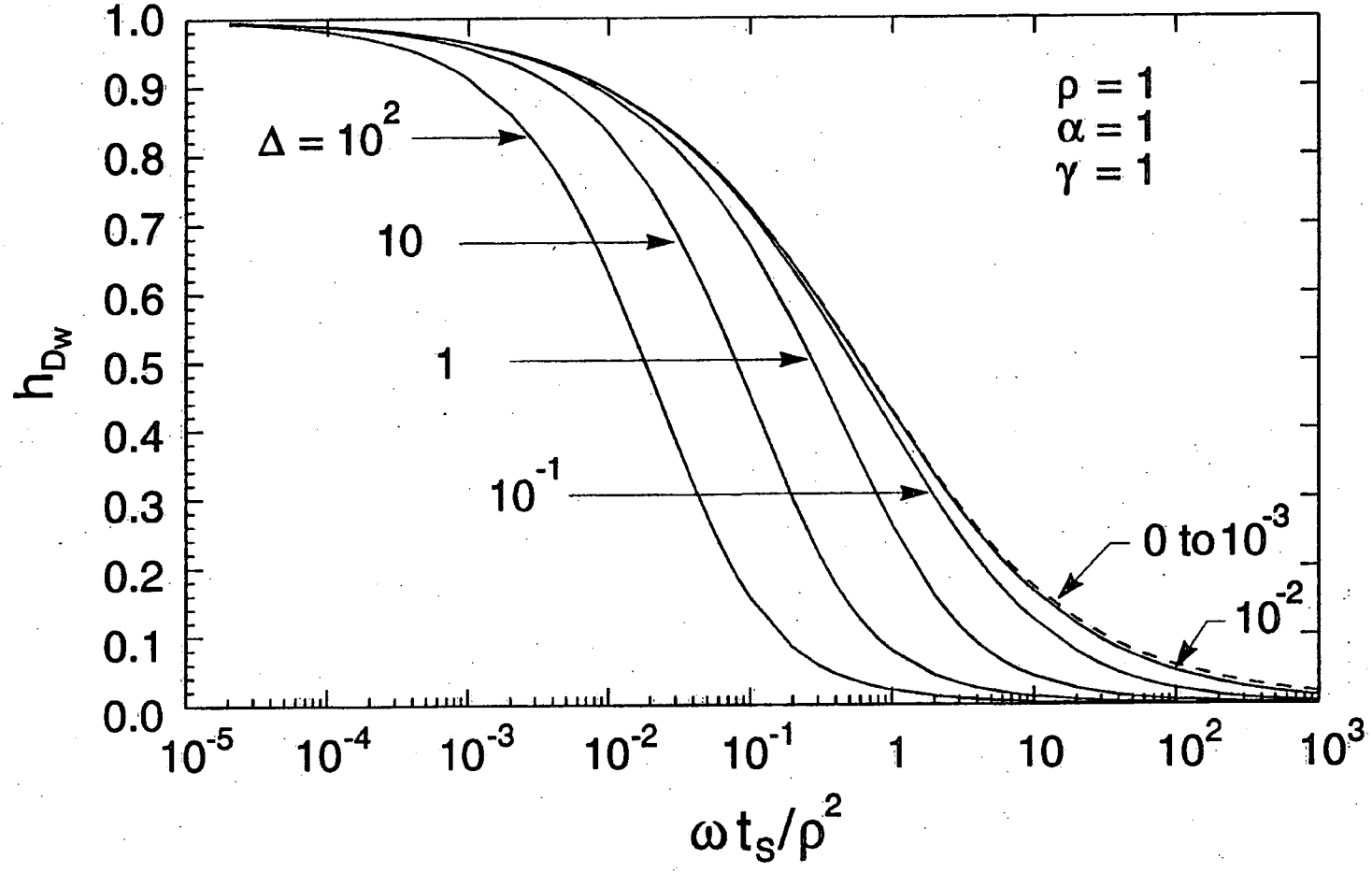

Figure 6. Intermediate time semilog type curves for a slug test in a fully penetrating wellbore with a permeable matrix. No skin is present (α and γ equal 1.0), Δ ranges from 0 to 10^2 (right to left), and ρ equals 1.0.

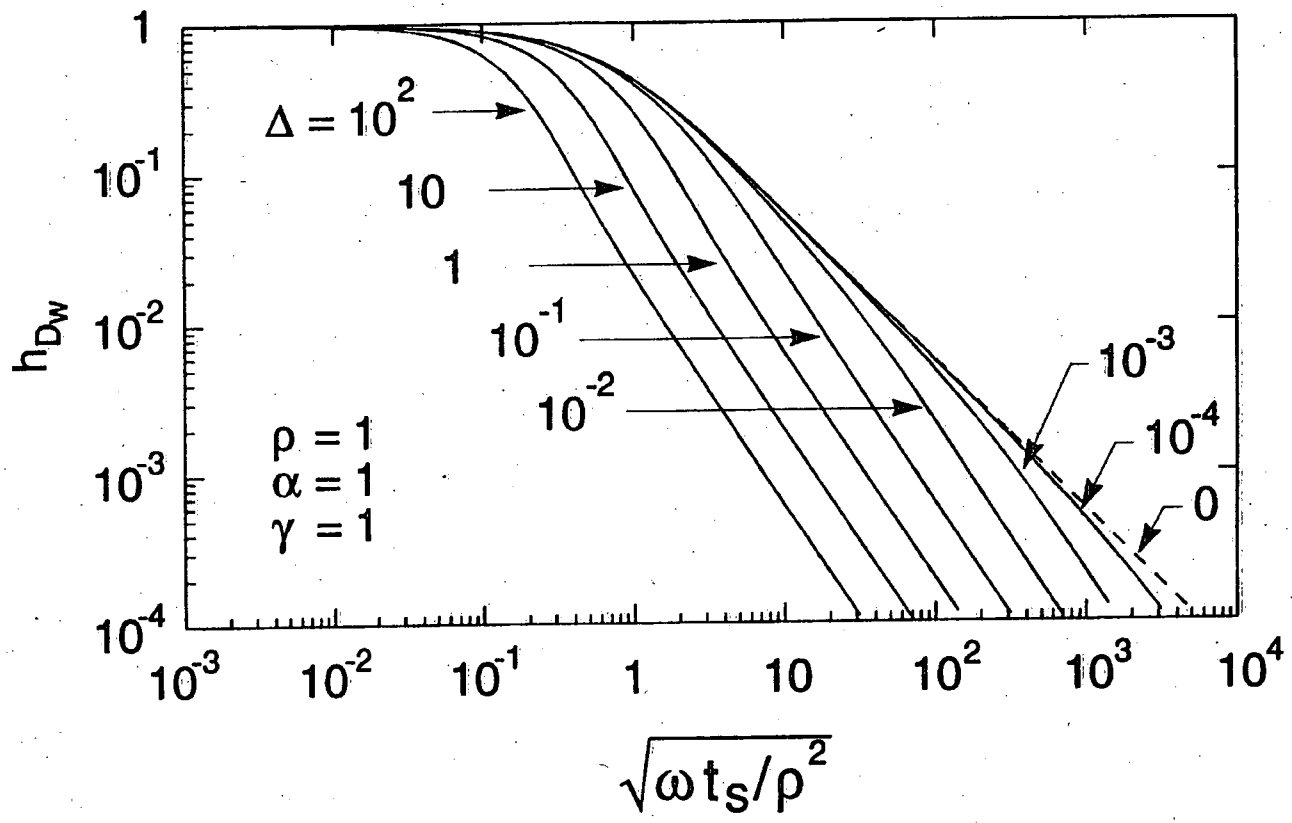

Figure 7. Log-log type curves for the late time response of a slug test in a fully penetrating wellbore with a permeable matrix. No skin is present (α and γ equal 1.0), Δ ranges from 0 to 10^2 (right to left), and ρ equals 1.0.

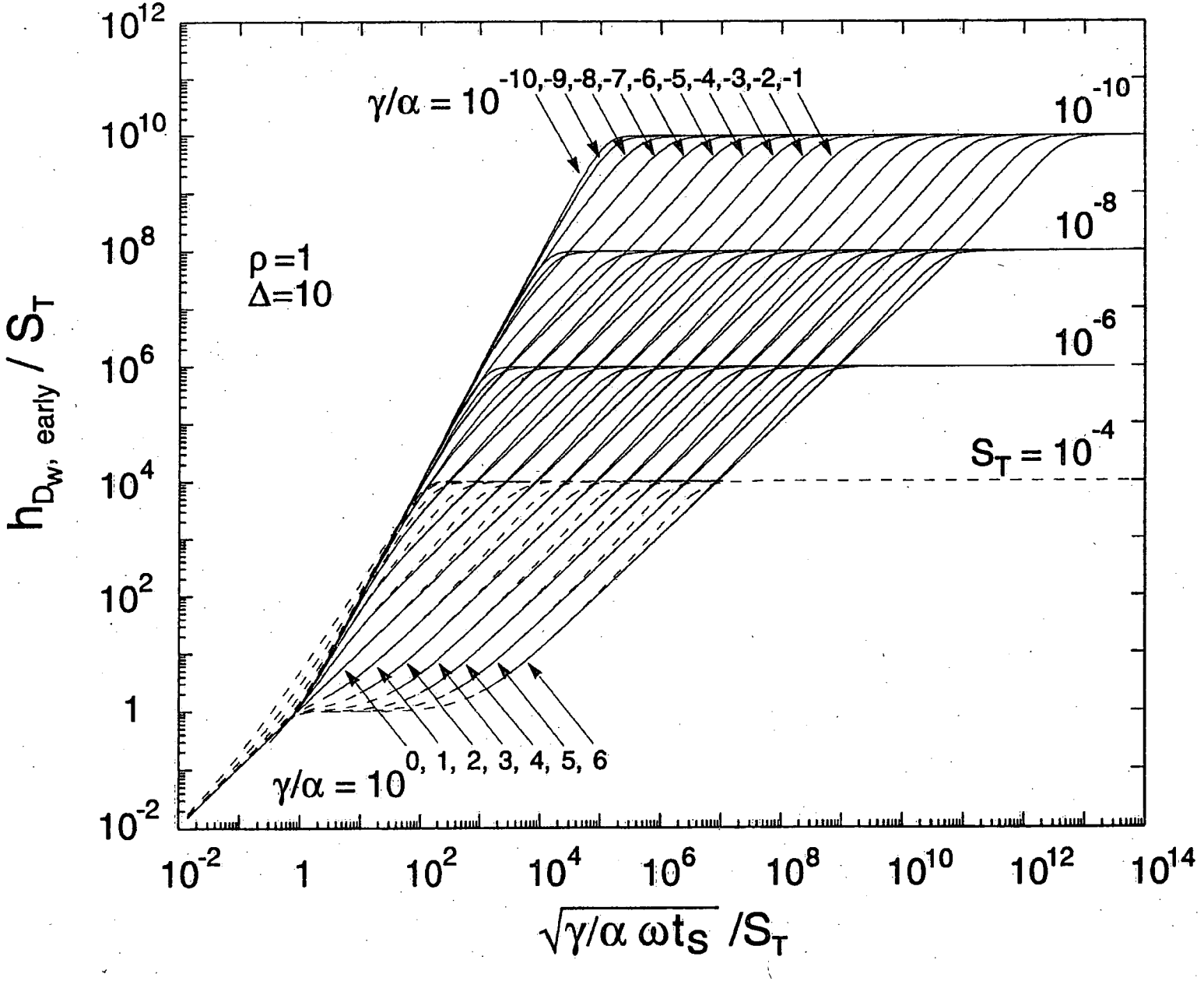

Figure 8. Log-log type curves for the early time response (normalized by $1/S_T$) of a slug test in a fully penetrating wellbore with a permeable matrix and a finite thickness skin. Curves are shown for γ/α ranging from 10^{-10} to 10^{6} (left to right), S_T ranging from 10^{-10} to 10^{-4} (top to bottom), ρ equal to 1.0, and Δ equal to 10.

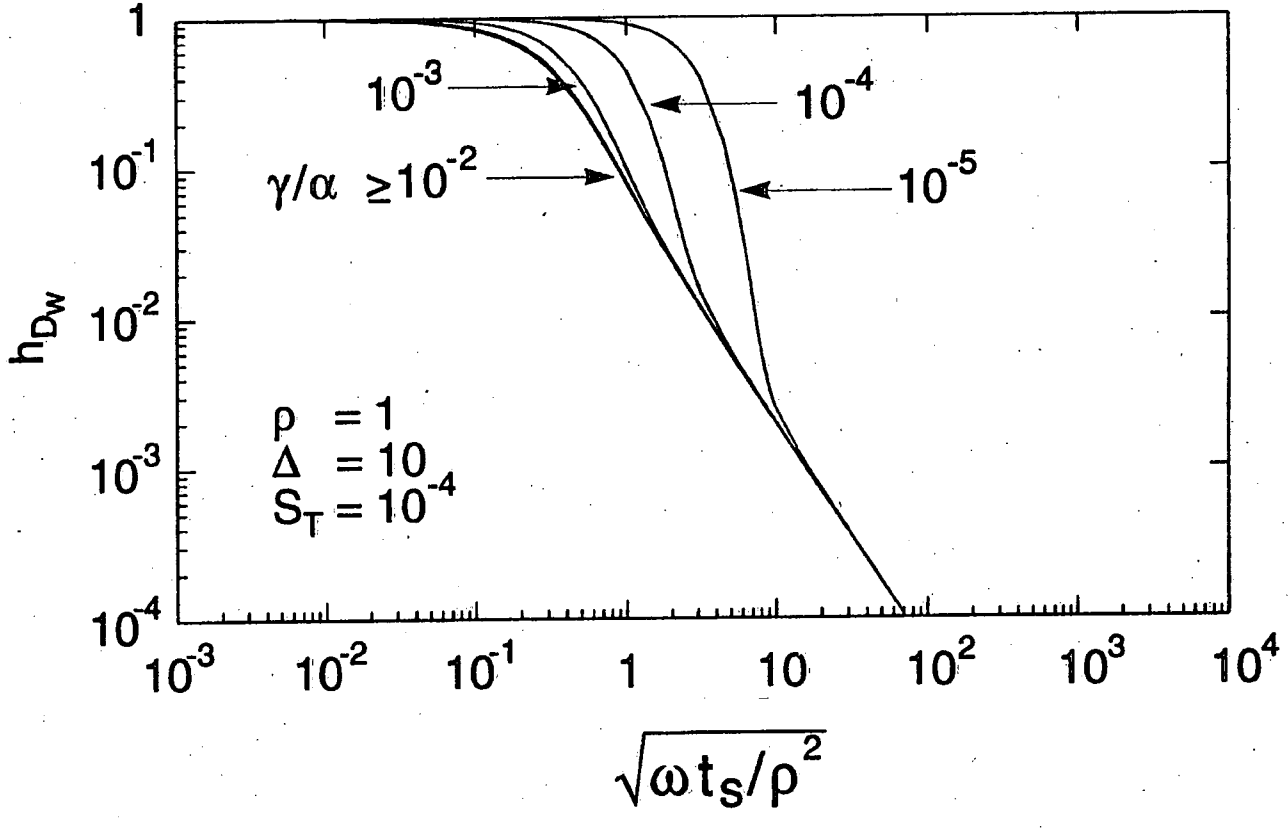

Figure 9. Log-log type curves for the late time response of a slug test in a fully penetrating wellbore with a permeable matrix and a finite thickness skin. Curves are shown for γ/α ranging from 10^{-5} to $\geq 10^{-2}$, S_T equal to 10^{-4}, ρ equal to 1.0, and equal Δ to 10.

PRINTED IN CANADA
IMPRIMÉ AU CANADA
ON RECYCLED PAPER
SUR DU PAPIER RECYCLÉ

National Water Research Institute
Environment Canada
Canada Centre for Inland Waters
P.O. Box 5050
867 Lakeshore Road
Burlington, Ontario
L7R 4A6 Canada

National Hydrology Research Centre
11 Innovation Boulevard
Saskatoon, Saskatchewan
S7N 3H5 Canada

NATIONAL WATER RESEARCH INSTITUTE
INSTITUT NATIONAL DE RECHERCHE SUR LES EAUX

Institut national de recherche sur les eaux
Environnement Canada
Centre canadien des eaux intérieures
Case postale 5050
867, chemin Lakeshore
Burlington, Ontario
L7R 4A6 Canada

Centre national de recherche en hydrologie
11, boul. Innovation
Saskatoon, Saskatchewan
S7N 3H5 Canada

Environment Canada Environnement Canada

Canada